Dissociation dynamics on ordered surface alloys

1999 J. Phys.: Condens. Matter 11 8397

(http://iopscience.iop.org/0953-8984/11/43/303)

J. Phys.: Condens. Matter **11** (1999) 8397–8415. Printed in the UK PII: S0953-8984(99)04944-9

Dissociation dynamics on ordered surface alloys

B E Hayden† and A Hodgson‡

† Department of Chemistry, The University of Southampton, Southampton SO17 1BJ, UK
‡ Surface Science Research Centre, The University of Liverpool, Liverpool L69 3BX, UK

Received 7 June 1999

Abstract. There are a number of well characterized single crystal alloy surfaces for which the dynamics and kinetics of dissociative adsorption has been investigated. We compare results for hydrogen and nitrogen dissociation on a series of such alloy surfaces, where the dynamics of dissociation has also been characterized on the surfaces of the pure components. Through a consideration of the electronic structures of the systems and the ground state adsorption energetics of the molecular (reactant) and dissociated (product) states, we investigate the influence of geometric and electronic effects in alloying on the region of the potential energy surface relevant to dissociation. We show that for direct dissociation there is in general a correspondence between the adsorption energetics on some local ensemble and the activation energies to dissociation. In some cases it is possible to relate the change in the adsorption barrier, and the product binding energy, to a modification of the electronic structure caused by alloying. It is more difficult, however, to establish the contribution of electronic perturbation to modification of a reaction ensemble for dissociation which involves more than one of the component atoms. These changes can result in concomitant changes in an individual dissociation channel. We also highlight dynamical effects caused by alloying which modify the pre-exponential (steric) factor for dissociative adsorption in addition to the change in the number of active sites.

1. Introduction

Alloying metals has long been exploited as a way of modifying the reactivity of surfaces, allowing the thermodynamic properties of adsorbates to be adjusted and providing a route to optimize the kinetics and selectivity of catalytic systems. A considerable experimental effort has been made to determine the effect on adsorption and reactivity of systematically modifying the composition of heterogeneous alloy catalysts [1, 2] and was supported at the time by the development of electronic structure calculations [3]. While such materials are often complex, multi-component systems, ordered bimetallic surface alloys offer an opportunity for detailed experiments to determine the influence of alloying on electronic structure and adsorption behaviour. These studies can be extended to investigate the dynamics of adsorption and the recombination kinetics, key elementary steps in surface reactions.

The mechanism by which surface reactivity is modified by alloying has traditionally been divided into two components [4, 5]. Firstly alloying may modify the adsorption energetics and concomitantly the barrier for reaction (e.g. dissociation), by perturbing the electronic structure of the surface, the so called 'ligand effect'. This effect may be local to an alloying atom, or may be longer range, the surface behaving homogeneously. Secondly, the introduction of different species into a surface creates chemically different sites on the surface, the so called 'ensemble effect'. This provides a range of different sites for adsorption, and hence will also change the distribution of transition states available for reaction or dissociation. It is

0953-8984/99/438397+19$30.00

important to note that both ligand and ensemble effects can modify the kinetics and dynamics of surface reactions by perturbing either the adsorbed reactant (e.g. a molecular state) or the adsorbed product (e.g. dissociative state). The dissociation dynamics will show very different behaviour depending on whether the modification occurs primarily in the entrance channel for reaction, as the reactant approaches the surface, or in the exit channel as the atoms dissociate, leading to different predictions about the reactivity. In addition there are other, less directly controllable factors which may influence the activity of alloy surfaces. For example the surface may respond to adsorption of a gas by restructuring, or by the segregation of one component to the surface, resulting in a change in reactivity of the alloy in the presence of an adsorbate [6, 7]. In such cases obtaining a detailed picture of how the ensemble and ligand effects influence adsorption and reaction is complicated by the problem of determining the surface structure and composition.

Creation of an *ordered alloy surface* forms a series of distinct sites on the surface, whose chemical character is different from that of the pure metal surface. We will concentrate on the effect of creating such sites on the dynamics of dissociation, one of the simplest and arguably one of the most important elementary steps in a catalytic reaction. Because of its simple interaction with metal surfaces, hydrogen dissociation provides an interesting probe of alloy reactivity. Dissociation may proceed either directly without a barrier on the more reactive transition metals, or via a barrier to dissociation on the noble and simple metals [8]. The low mass of the adsorbate, the small physisorption interaction and the absence of a stable molecular well all combine to make the dissociation process direct and trapping into molecular states can usually be ignored. One benefit of this for investigating alloy reactivity is that the barrier to dissociation is very dependent on the final state energetics. For example, Feibelman [9] showed that the most favourable dissociation sites on Rh(100) were those sites where the H atoms could be brought into a stable binding geometry without requiring a large, energetically costly, extension of the H_2 bond. In these circumstances the barrier height is closely related to the binding energy of the H atoms, an observation supported by looking at the variation of barrier height with site on other surfaces, such as Cu [10–12]. This means that for H_2 dissociation on ordered alloy surfaces we may be able to make a direct correlation between the favourable binding sites available for H and the size of the barrier to dissociative chemisorption. On metals where there is no barrier to dissociation, such as Pd [13] and W [14, 15], the reaction cross section will be sensitive to the form of the attractive well which steers the reactant molecule into a favourable geometry to dissociate [16, 17]. In this case the effect of changing an alloy site may be more difficult to anticipate.

When discussing the reactivity of alloy surfaces it is often useful to think of changes in reactivity as originating entirely from either the ensemble or the ligand effects, as if they were two completely distinct and different factors. Thus it might be possible to explain the changes in reactivity as determined on the basis of an ensemble mechanism, where the formation of an alloy creates a number of different chemical sites on the surface, without explicitly including any ligand effect. In this model each type of chemically distinct site created on the surface has a different reactivity compared to the original surface, but the reactivity of equivalent local sites is not dependent on the composition of the rest of the surface. Such a model implicitly includes local electronic effects, which modify the reactivity of particular dissociation sites, but ignores indirect ligand effects caused by alloy atoms outside some critical local group. Clearly the ensemble and ligand effects must generally occur together and distinguishing the two as independent entities is impossible. Nevertheless, it is often useful conceptually to assume that such a separation is valid and then to investigate how well the approximation holds. In particular, if the principal influence on reactivity occurs via the ensemble effect, the reactivity depending on the distribution of new chemical sites on the surface with that of the individual

metals remaining similar to that of the pure surfaces, then it will often be possible to extrapolate the reactivity of the alloy surface from that of the pure materials. If, on the other hand, the reactivity of one component changes substantially due to its local electronic environment, for example if an activation barrier disappears and dissociation becomes non-activated (or vice versa), then simple, intuitive chemical predictions about the alloy reactivity will fail and it will be necessary to correlate this to the local electronic structure, for example using a DFT calculation or equivalent [18].

While the separation into ligand and ensemble factors may be convenient from a conceptual or intuitive standpoint, it is otherwise somewhat arbitrary; there is no simple experimental test which will immediately reveal whether a change of reactivity is due to one effect or the other. However, kinetic or dynamic measurements do provide information about the magnitude of energy barriers and the steric requirements for adsorption and desorption. Both of these factors can be modified either by electronic effects changing the local potential in the region of one of the atomic components or by the creation of different sites on the surface. However, in some cases, for example where we can obtain sufficient control over the alloy that we can make different, well defined reaction sites, it may be possible to argue from the accumulation of evidence which factor is dominant. For example, we may be able to assume, as a first simple model, that each dissociation site is characterized by a particular activation barrier which depends only on the local ensemble of atoms, with electronic effects being less important. Large changes to the activation energy can then be associated with a change in the site for dissociation, while changes to the steric factor will reflect the number of sites available and any change in the entropic constraints on the transition state geometry induced by alloying. By changing the sites available on an ordered alloy we can investigate whether the reactivity is consistent with this simple site picture, or whether the change in reactivity is determined by electronic effects.

A number of dynamical and theoretical studies have recently been published concerning the dissociation of small molecules on well characterized alloy surfaces. Here we review the different ways in which alloying can modify the dissociation dynamics of small diatomic molecules, specifically hydrogen and nitrogen, restricting the discussion to alloy surfaces where the geometric arrangement of metal atoms is well defined and where the surface does not reconstruct or segregate upon adsorption. We will concentrate on evidence of how the form of the potential energy surface for dissociative chemisorption is modified, describing recent results for ordered alloy surfaces in the light of the chemisorption properties of molecular and dissociative states on pure metal surfaces and the electronic structure of the alloys through theoretical calculations. We will review evidence as to how changes to the electronic structure and the available dissociation sites modify the barrier to dissociation in different alloy systems. In doing so we will discuss to what extent experimental measurements, which provide information about energy barriers and steric factors, can distinguish the origin of a change in reactivity. We will describe simple geometric site arguments which can explain differences in reactivity in many of these systems and discuss criteria for when we should expect intuitive chemical pictures based on simple ensemble models to break down, and indirect electronic (ligand) effects to become more important. Finally we describe the dynamical features we expect to appear on alloy surfaces, caused by the spatial localization of dissociation sites on the surface, and discuss what can be learnt about molecular dissociation by investigating ordered alloy surfaces.

2. Dissociation at alloy surfaces

In the following sections we consider recent dynamical experiments on hydrogen and nitrogen dissociation at alloy surfaces. These experiments are grouped into two sections, based on

the reactivity of the majority metal. The first sections look at an inert metal, in this case copper, alloyed with more reactive metals such as Pt and Pd, while the second group looks at dissociation on reactive metals, such as W and Pt, alloyed with an inert metal such as Sn or Cu. In each case the dissociation behaviour of the pure metal surface is briefly reviewed first.

2.1. Hydrogen dissociation on noble and transition metals

Hydrogen shows a large activation barrier to dissociation on both the noble metals Cu [19–21], Ag [22, 23] and Au [24], as well as on the simple metals, such as Al [25], which have no accessible d bands. At low coverages on Cu(110) and Cu(100) the most stable atomic site appears to be the highest co-ordination available [26], although reconstruction of both surfaces at higher coverages results in changes to the adsorption site. Similarly, adsorption on Cu(111) populates the threefold hollow sites [27] and desorption is found to be second order, with an activation energy for desorption of 0.7 eV on Cu(111) and 0.5 eV on Cu(100) [20].

Hydrogen dissociation on copper surfaces has provided a model system for studying the dynamics of dissociative adsorption [28, 29]. It has been shown, both experimentally and theoretically, to be highly activated on Cu(111), Cu(110) and Cu(100), with translation and vibration being equally effective in accessing the seam in a direct process [19, 21]. Dissociation on Cu(111) is roughly thermoneutral with a barrier of $\sim$0.6 eV [20, 21], while dissociation on the other noble metals shows a larger barrier, $\sim$1.5 eV on Ag [30, 31] with the barrier on Al being sufficiently large that adsorption is dominated by atoms [25]. Density functional theory (DFT) calculations show the barrier to dissociation on Cu is displaced slightly into the exit channel, at extended H_2 separations [10–12, 32, 33]. The lowest energy barrier on Cu(100) is found for geometries with the molecular axis parallel to the surface at the fourfold or bridged sites in the unit cell, being $\sim$20 meV/molecule lower on the latter site [11, 27]. On Cu(111) the minimum energy path has hydrogen at a bridge site with the atoms dissociating into the stable threefold hollow sites [12]. The size of the barrier at different sites on the surface correlates closely with the binding energy of atomic H at those adsorption sites which form the transition state [10, 11]. This behaviour was described by Feibelman [9], who pointed out that the barrier to dissociation would be lowest for geometries where the H atom is bound tightly to the surface without breaking the H_2 bond (which is energetically expensive). Since H binds better at hollow or bridge sites this favours geometries where the H atoms lie close to high co-ordination sites for the equilibrium H_2 separation, making a low symmetry bridge site favourable for H_2 dissociation on Rh(100) [9]. Similar behaviour is also seen for H_2 dissociation at Ag(100) [34], where again the barrier to dissociation is large ($\sim$1.3 eV), occurs late in the reaction path and is correlated to the energy of the final binding site on the surface. Thus for dissociation over an activation barrier we expect the final state energy to be a qualitative guide as to which dissociation sites are favoured for hydrogen.

The large barrier to dissociation on the noble metals, as compared to the transition metals, was originally attributed to the cost of the repulsive interaction between the filled H_2 (σ_g) and the Cu sp orbitals [35]. On transition metal surfaces, which have partially filled d bands, the electron density is able to rehybridize to minimize the repulsion without a large cost in energy, resulting in a negligible barrier to dissociation on metals such as Ni [13], Pt [36] and Pd. This channel is not available on the simple or noble metals which have large barriers to dissociation. Hammer *et al* [24, 37] have recently reinvestigated the influence of electronic structure on the barrier to reaction using density functional theory. By projecting out the density of states at the transition state they argued that the height of the barrier was more closely correlated with the filling of the {$H_2(\sigma_g)$–metal d-band} antibonding orbital at the transition state, rather than simply the presence of holes in the metal d band or the density of states at the Fermi level.

When the d bands were sufficiently low lying that this antibonding orbital was filled at the transition state, dissociation became activated. Since this picture requires a DFT calculation of the local electronic structure, it does not provide a particularly simple model for differences in reactivity. However, it does provide a useful model for understanding the way in which the electronic structure can influence the barrier to dissociation at a particular metal site.

2.2. Hydrogen dissociation on CuPt alloys

The Cu_3Pt system forms an ordered CuPt(111) surface alloy, with Pt atoms forming a (2×2) substitutional alloy in a Cu(111) surface, each Pt being completely surrounded by Cu [38]. Ion scattering measurements show that the Pt atoms lie coplanar with the Cu, with the equilibrium surface having slightly less Pt in the top layer than expected for the ideal (2×2) structure and a corresponding increase in the second layer. The surface therefore consists of an array of isolated Pt atoms, 5.2 Å apart in a Cu matrix, giving a well defined surface for adsorption measurements (figure 1). Pt is an active catalyst for hydrogen dissociation, the Pt(111) surface [36] showing a sticking probability that increases steadily with energy, without an energy threshold, indicating that some adsorption geometry exists for which the barrier to dissociation is negligible.

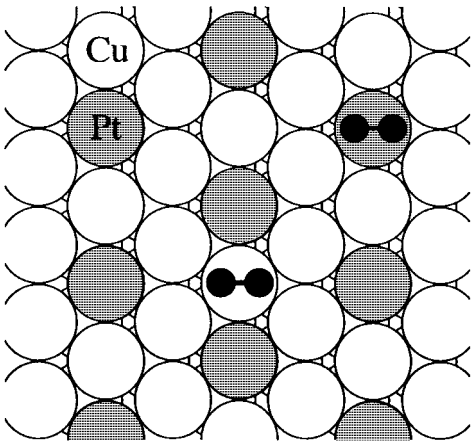

Figure 1. The Cu(111)–p(2×2)Pt surface showing the presence of isolated Pt atoms some 5.2 Å apart in a Cu matrix. Hydrogen is shown in the atop to hollow dissociation geometries calculated in [18].

Wandelt and co-workers [39] have looked at H_2 dissociation on the Cu(111)–(2×2)Pt surface and find reaction efficient, uptake saturating after a dose of just 5 L of hydrogen. The low exposure required to saturate the surface indicates that dissociation is non-activated, while UPS results suggest that H atoms are bound on the Pt, blocking these sites and preventing further adsorption. Since the Cu surface has a barrier of $\sim$0.6 eV, the absence of any barrier to dissociation implies that isolated Pt atoms in the Cu matrix provide sites which are able to dissociate H_2 [39]. This was supported by the observation that dissociation could be blocked by pre-adsorbing CO on the surface, the CO occupying the Pt sites and preventing hydrogen dissociation.

Hammer and Nørskov [18] looked at the influence of electronic structure on dissociation at the $Cu_3Pt(111)$ surface using a density functional calculation. They compared atop to hollow dissociation over a Pt or Cu atom in an unrelaxed $Cu_3Pt(111)$ surface (figure 1) with dissociation at the same site in the pure metal. Dissociation over Cu into the threefold Cu

sites was activated, just as on Cu(111), while the Pt site (where H dissociates into a Cu_2Pt threefold hollow site) showed no barrier to dissociation, just as on pure Pt(111). As discussed above, the difference in reactivity of the Cu and Pt sites was attributed to the energy of the $\{\sigma_g$–d$\}$ antibonding orbital, since neither site had significantly different d band filling or DOS at the Fermi level. This calculation did not report the influence of the final binding site (Cu_3 or Cu_2Pt hollow site) on the barrier for dissociation at Cu.

2.3. Hydrogen dissociation on CuPd alloys

Hydrogen dissociation on CuPd alloys provides a contrast to the CuPt system. The d band of Pd is very nearly full and requires only a small charge exchange from the second component of the alloy to completely fill the band [40]. Hydrogen dissociation on the ordered $Cu_{85}Pd_{15}(110)$ surface has been studied by molecular beam adsorption [41]. This crystal forms an ordered surface in which the top later is entirely Cu(110) but the second layer contains 0.5 ML of Pd as a (2×1) layer of CuPd [42] (figure 2). The Pd content oscillates in subsequent layers until it reaches the bulk stoichiometry. Despite the availability of Pd in the second layer, the binding energy of H on this surface is very similar to that on Cu and dissociation is highly activated [41], the sticking probability being lower than that on Cu(110), and similar to that of Cu(111) (figure 3). Since there is no Pd in the top layer the sites available for dissociation have not changed and any reduction in the dissociation probability must be caused by a ligand effect.

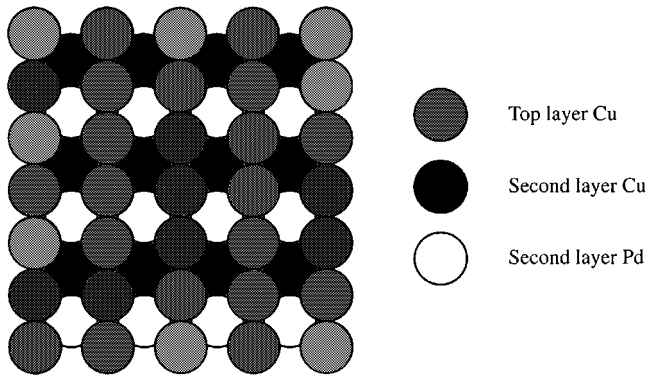

Figure 2. The ordered Cu(110)–(2×1)Pd surface showing the top layer of Cu overlaying a (2×1) layer containing 50% Pd [42].

CuPd alloys with larger Pd stoichiometries, $Cu_{50}Pd_{50}(111)$ [43] and $Cu_{25}Pd_{75}(111)$ [44], form disordered surfaces and hydrogen dissociation on these surfaces is non-activated. The saturation H coverage was sensitive to the Cu content of the surface, and it was argued that the adsorption behaviour was consistent with dissociation on Pd sites, H binding in threefold Pd sites and blocking further adsorption. Annealing the sputtered $Cu_{85}Pd_{15}(110)$ surface to a temperature below 500 K prevented complete segregation of Pd into the bulk and resulted in a disordered (1×1) surface with substantial Pd in the surface layer [45, 46]. In this case thermal desorption traces showed a second feature, associated with desorption of hydrogen from Pd islands in the surface, with a similar desorption temperature to that seen from Pd(111) [41]. The disordered surface showed a much higher initial dissociation probability, S_0 increasing slightly with energy in a manner similar to the behaviour on Pd surfaces. CuPd alloys have a large negative enthalpy of formation, the Pd preferring to be surrounded by Cu [44, 47], and it is possible to estimate the Pd concentration in the surface from simple pair models for

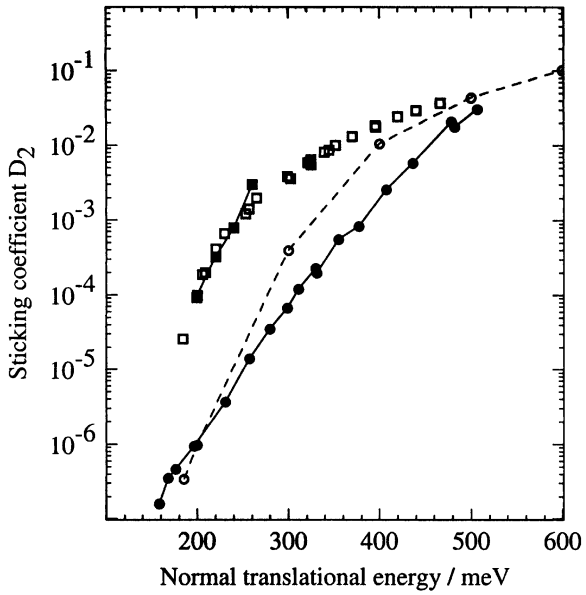

Figure 3. Sticking of D_2 on ordered Cu(110)–(2 × 1)Pd (●), Cu(111) [21] (dotted line) and Cu(110) surfaces (■ [20], □ [19]).

the Cu– Pd interaction potential, based on the temperature required to order Pd into the bulk. This indicates that even the ordered (2 × 1) surface will contain somewhere between 10^{-3} and 10^{-5} ML of Pd atoms. Since the sticking probability at low energy, $S < 1 \times 10^{-7}$ on the (2 × 1) surface, the remaining isolated Pd atoms in the top layer clearly do not dissociate H_2 efficiently, in contrast to the behaviour of isolated Pt atoms in $Cu_3Pt(111)$ [39]. The non-activated adsorption of H_2 on the higher Pd alloys [43, 44] is probably due to the presence of clusters of Pd atoms, just as for the disordered (1 × 1) $Cu_{85}Pd_{15}(110)$ surface.

2.4. Hydrogen dissociation on PtSn alloys

Tin forms a series of substitutional alloys with Pt and deuterium desorption from Pt(111), and Pt(111)–p(2 × 2)Sn and Pt(111)–($\sqrt{3} \times \sqrt{3}$)R30°Sn has been studied and activation energies (E_d) and pre-exponential factors (ν) obtained [48]. Desorption is found to follow second order kinetics, with the desorption parameters for the low coverage limit shown in table 1. The structures of the alloy surfaces are shown in figure 4. Since atomic hydrogen adsorbs in the threefold hollow site on Pt(111) [49, 50], it is perhaps not surprising that the largest change in the desorption parameters occurs when these sites are excluded by formation of the Pt(111)–($\sqrt{3} \times \sqrt{3}$)R30°Sn alloy. The desorption results can be related to measurements of sticking probabilities $S(E)$ through the principle of detailed balance. The Pt(111) surface exhibits a linear increase in sticking with translational energy from the lowest energies [36], figure 5. The Pt(111)–p(2 × 2)Sn surface also exhibits dissociation at low energies, sticking increasing linearly from the lowest energies, but with a much reduced (∼×30) probability. In addition, however, there is an activated component, characterized by an onset at ∼0.3 eV. Pt(111)–($\sqrt{3} \times \sqrt{3}$)R30°Sn does not show non-activated component, but displays a clear threshold to dissociation at around 0.3 eV, the same energy above which sticking increases abruptly for the (2 × 2) surface.

Table 1. Parameters for D_2 desorption and adsorption from SnPt alloys (see text for details).

	E_d (eV)	ν (cm^2/atom s^{-1})	E_a (eV)	E_{BE} (kJ mol^{-1})
Pt(111)	0.71	4×10^{-5}	0.03	251
Pt(111)–p(2 × 2)Sn	0.67	5×10^{-6}	0.03	249
Pt(111)–($\sqrt{3} \times \sqrt{3}$)R30°Sn	0.40	1.3×10^{-8}	0.28	224

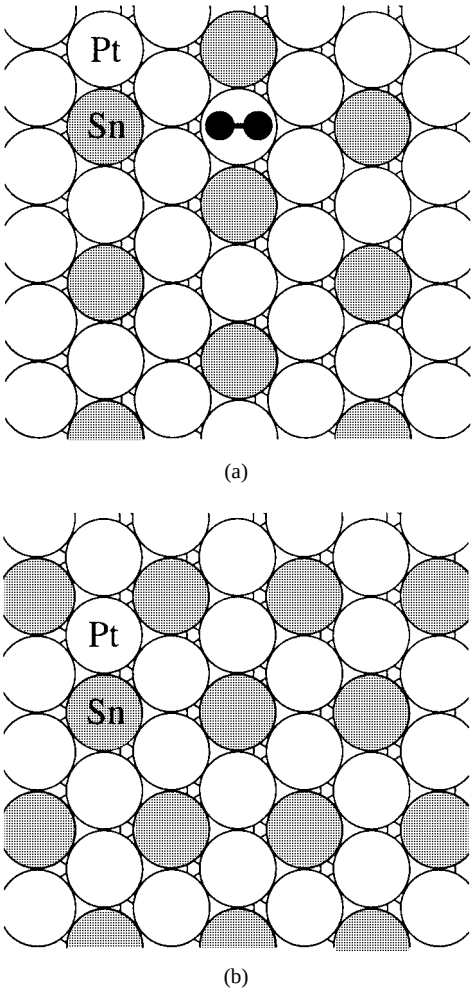

Figure 4. Structure of (a) the Pt(111)–p(2 × 2)Sn and (b) the Pt(111)–($\sqrt{3} \times \sqrt{3}$)R30°Sn surface alloys. The favoured atop to hollow dissociation site for H_2 on the Pt(111) surface is shown on the Pt(111)–p(2 × 2)Sn alloy but is not available on the ($\sqrt{3} \times \sqrt{3}$)R30°Sn surface where the Pt_3 clusters are lost by alloying.

An estimate of the binding energy of the dissociative state can be obtained by comparing the barriers to dissociative chemisorption and recombinative desorption. The Arrhenius activation energy for dissociative adsorption (E_a) is obtained by integrating the sticking probability over an isotropic Maxwellian energy distribution at the temperature where desorption occurs. In this way the atomic binding energy can be estimated [48], and values for the three surfaces are

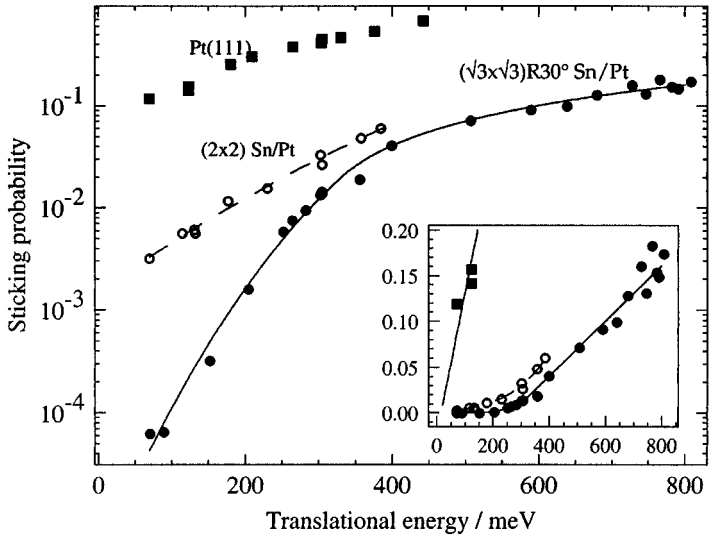

Figure 5. Logarithmic plot showing the sticking probabilities for D_2 on the Pt(111) (■), p(2×2)Sn (○) and Pt(111)–p($\sqrt{3} \times \sqrt{3}$)R30°Sn (●) surface alloys. The inset shows the sticking for large *S* as a linear plot, revealing the threshold behaviour shown by the alloy surfaces.

included in table 1. The presence of Sn adjacent to the Pt_3 ensembles on the Pt(111)–p(2×2)Sn surface (figure 4) evidently has a minimal effect on the electronic structure of the D binding sites. However, the change in D binding energy correlates well with the presence of the threefold hollow site, which is removed on Pt(111)–($\sqrt{3} \times \sqrt{3}$)R30°Sn. The hollow site ensemble is now Pt_2Sn, with the heat of adsorption dropping by ∼0.5 eV (table 1) and dissociation becoming almost thermoneutral. It is not certain whether the binding site remains the hollow site on the Pt(111)–($\sqrt{3} \times \sqrt{3}$)R30°Sn surface, and there is some indication from core level photoemission [51] that H may prefer to adsorb atop the Pt atoms on this surface.

It is clear that there is an abrupt increase in the activation barrier to dissociation on the Pt(111)–($\sqrt{3} \times \sqrt{3}$)R30°Sn surface, concomitant with the change in binding energy of the dissociative state. The sticking dependence on Pt(111)–p(2 × 2)Sn appears (above) to be a combination of Pt(111) type behaviour (low activation barrier but with reduced probability) and Pt(111)–($\sqrt{3} \times \sqrt{3}$)R30°Sn behaviour (highly activated) at higher energies. This can be interpreted in terms of the heterogeneous distribution of sites on Pt(111)–p(2 × 2)Sn, which exhibits both Pt_3 and Pt_2Sn ensembles (figure 4). On Pt(111) DFT calculations find the optimum path for dissociation to be the atop to threefold hollow geometry, the H atoms dissociating directly into the stable threefold hollow site [18]. This path is non-activated on Pt(111) and the same ensemble is present on Pt(111)–p(2×2)Sn, with a very similar final state binding energy (table 1). The p(2 × 2)Sn surface also shows a non-activated component, but this is lost on Pt(111)–($\sqrt{3} \times \sqrt{3}$)R30°Sn which shows only activated adsorption. If we pursue the idea of favoured dissociation sites being correlated with the binding energy of the H atoms at the transition state [9] then we can speculate on the site responsible for dissociation above 290 meV on Pt(111)–($\sqrt{3} \times \sqrt{3}$)R30°Sn. Since H prefers to bind to Pt in high co-ordination sites, the adsorption site on Pt(111)–($\sqrt{3} \times \sqrt{3}$)R30°Sn is likely to be either the Pt_2Sn hollow or the Pt_2 bridge site. Dissociation paths which lead directly to these binding geometries are the PtSn bridge to hollow geometry and the nearby C_{2v} geometry with H dissociating directly into the Pt bridge site. Both of these sites also exist on the Pt(111)–p(2 × 2)Sn alloy and indeed

$S(E)$ for the (2×2) alloy can be reproduced by combining the non-activated behaviour, characteristic of the Pt_3 ensembles, and the activated behaviour channel characteristic of the Pt_2Sn ensembles of the Pt(111)–$(\sqrt{3} \times \sqrt{3})$R30°Sn alloy. Thus this simple model of the adsorption process, in terms of the local ensemble of atoms adjacent to the stable H binding sites, gives a consistent picture of the energy dependence of dissociation at these alloys. What it does not account for is the relative importance of each channel or steric constraints on the transition state at the alloy surface.

2.5. Pre-exponential and steric requirements for dissociation on Sn/Pt

Formation of the SnPt alloys (figure 4) creates surfaces which, even if macroscopically flat with minimal vertical distortion of the overlayer, will show a strong corrugation of the activation barrier to dissociative chemisorption. This localization will show up as a change in the pre-exponential (steric) factor in adsorption or desorption, but may also be seen directly in changes to the energy scaling and how the translational energy parallel and perpendicular to the surface contributes to overcoming the barrier to dissociative chemisorption.

Activated dissociative chemisorption of diatomic molecules often follows a normal energy scaling, the dissociation probability being dependent only on the component of the translational energy perpendicular to the surface. This energy scaling is consistent with a potential energy surface for dissociation which has no lateral site dependence, and therefore cannot mix motion parallel to the surface into the dissociation co-ordinate. In this case the surface can be represented by a jellium model and low dimensional models which ignore the lateral corrugation of the potential are adequate. The introduction of a corrugation in the barrier to dissociation changes the energy scaling, allowing motion parallel to the surface to influence the dissociation probability. The corrugation can be broken down into two different components, a lateral variation in the magnitude of the barrier, referred to as an energetic corrugation, and a change in the vertical location of the barrier across the unit cell or geometric corrugation [52, 53]. These are shown schematically in figure 6 and give rise to rather different energy scaling behaviour with incidence angle, θ. In the case of a localized barrier, a molecule moving parallel to the surface will be carried past the favourable dissociation site, resulting in a reduction in the sticking probability when this motion becomes sufficient to take a molecule from a favoured geometry to a repulsive site before dissociation is complete. A good example of this is the behaviour seen for H_2 dissociation on Fe(110), where below 0.25 eV the sticking probability is strongly inhibited by motion parallel to the surface, consistent with a localized dissociation site [54, 55]. If instead the vertical location of the barrier above the surface changes with site then motion parallel to the surface can couple to the dissociation co-ordinate and aid sticking. In some cases these two effects may counter-balance, and this may be used to explain the approximately normal energy scaling for H_2 dissociation on Cu(111) at energies near the sticking threshold [52]. However, even in this case desorption departs from a normal energy scaling as the translational energy is dropped below the barrier height and all of the energy begins to contribute to dissociation [56].

Now for an alloy surface comprised of one reactive and one unreactive metal, we expect the magnitude of the barrier to be highly corrugated, reflecting the different chemical environments, even when the surface remains physically flat. This will give rise to a strong lateral site dependent corrugation which should be visible in molecular beam adsorption measurements when dissociation is direct and activated. A good example of such a system is dissociation on the Pt(111)–$(\sqrt{3} \times \sqrt{3})$R30°Sn surface. Whereas the Pt(111) surface shows dissociative chemisorption of H_2 even at low translational energy, the $\sqrt{3}$ surface has a substantial activation barrier to sticking with the dissociation probability falling exponentially below $\sim$0.3 eV.

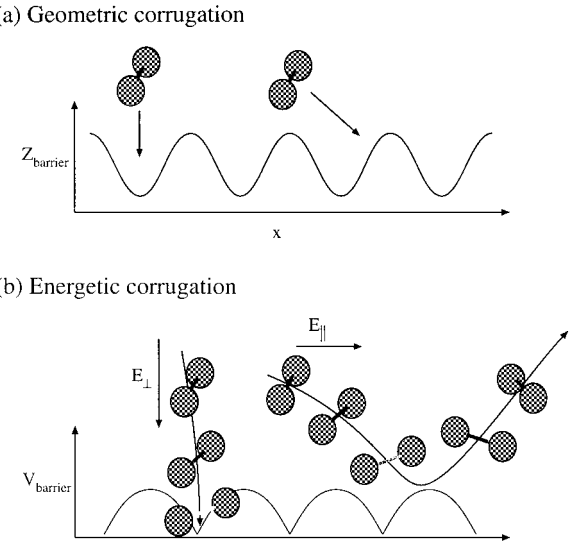

Figure 6. The corrugation of the barrier to dissociation can be broken down into two different components which are shown schematically, (a) a change in the vertical location of the barrier across the unit cell (geometric corrugation) and (b) a lateral variation in the magnitude of the barrier with site (energetic corrugation). In the case of a geometric corrugation motion parallel to the surface can assist dissociation whereas for the energetic corrugation motion parallel to the surface inhibits dissociation by carrying the molecule away from a favoured dissociation site [52, 53].

Although sticking on a clean Pt(111) surface does not depart greatly from normal energy scaling [36], bringing the H_2 molecules in at an angle to the alloy surface normal results in a strong suppression of dissociation, figure 7. This is consistent with the presence of a localized dissociation site on the surface, motion parallel to the surface hindering sticking by taking the molecule away from a favoured site, as described above [54, 55].

2.6. Hydrogen dissociation on CuW

Hydrogen dissociation on tungsten is facile, with significant probabilities of dissociation at very low incident energies. Both indirect and direct channels have been proposed to explain the incident beam energy dependence on W(100) [14, 15], although the low energy component has also been ascribed to a steering effect at low translational energies [17]. What is clear is that dissociation is effectively non-activated. There have been no chemisorbed molecular states found experimentally, and this is also apparent in the PES generated by density functional calculations [57]. Dissociative adsorption on W(100) leads to surface reconstruction and atomic hydrogen adsorption in bridged sites at low coverages, while tungsten bridge sites are also occupied in the saturation overlayer of 2 ML in a W(100)–(1×1) structure [58]. DFT calculations find the adsorption energy greatest in the twofold bridged sites at 0.95 eV/atom [57], 0.4 eV and 0.7 eV more stable than the hollow and on top sites respectively, and in good agreement with the experimental value of 0.825 eV/atom [59]. The most favourable site and geometry for dissociation is found to be the atop site, with the molecular axis in the plane of the bridged sites, although there is no barrier to dissociation over much of the surface.

The W(100)–c(2×2)Cu alloy surface has the structure shown in figure 8 and has lost all the favoured W–W bridging sites for the dissociative state [60]. The β_1 and β_2 desorption peaks at 435 K and 525 K of hydrogen on W(100) are replaced by a desorption state at 265 K

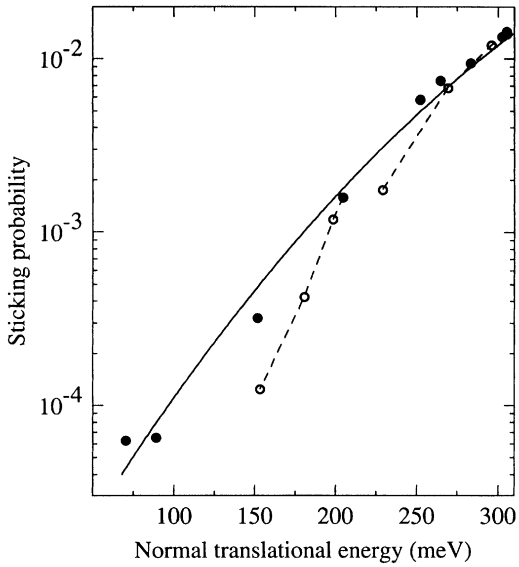

Figure 7. Sticking on the Pt(111)–($\sqrt{3}\times\sqrt{3}$)R30°Sn surface as a function of the normal component of the translational energy ($E\cos^2\theta$) for $E < 0.3$ eV. The angular dependence is shown (open symbols and dotted lines) for increasing angle at two fixed translational energies, 0.2 and 0.3 eV. For a given normal energy sticking is lower for molecules which are also moving parallel to the surface.

on the alloy [61], which can be compared to a desorption temperature of ∼320 K on Cu(110) [62]. The translational energy dependence of dissociative sticking on W(100) [14, 15] and W(100)–c(2 × 2)Cu [61] is shown in figure 9. The result on the alloy surface has been interpreted in terms of an increase in the barrier to direct dissociation over that of the W(100) surface; the onset of sticking at ∼150 meV on the alloy is due to translational activation in a direct process. This is supported by a surface temperature independence, and a linear decrease with hydrogen coverage for this high energy channel. In contrast the low energy channel, while exhibiting only a small temperature dependence, shows a coverage dependence characteristic of an indirect channel. This has been ascribed to indirect dissociation at defects which appear to exist at similar concentrations on both the W(100) and W(100)–c(2 × 2)Cu surfaces. Subtraction of the indirect channel contribution to the sticking data on W(100) and W(100)–c(2 × 2)Cu allows a comparison of the barriers to dissociation via the direct channel on these surfaces, and a comparison to the same channel on Cu(110) (figure 10). S_0 on W(100) exhibits a linear rise from 10^{-2} at 0 meV to 0.6 at 350 meV, and is very similar to the form of the curves obtained on the H_2–Fe [54] and H_2–Pt [36] systems in the absence of step defects which result in an additional low energy channel [63]. The size of the barrier to direct dissociation on the W(100)–c(2 × 2)Cu surface is thus intermediate between the two extreme cases of non-activated dissociation on tungsten, and high activation on copper. This could be a result of either geometric or electronic effects, or of course a combination of both. If the electronic structures (in particular the density of states in the d orbitals in the region of the Fermi level) of the two metals are altered by the bonding between them to produce a hybrid surface electronic structure, then the approaching hydrogen molecule would experience some intermediate tungsten–copper potential, irrespective of the collision site. The second possibility is that the specific dissociation site involves both unperturbed copper and tungsten atoms, so influencing the PES in the region of the barrier.

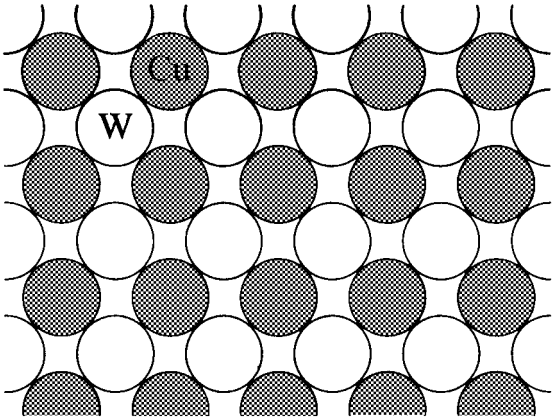

Figure 8. Formation of the W(100)–c(2 × 2)Cu alloy removes the W bridge sites favoured for chemisorption of H and the N fourfold hollow binding sites.

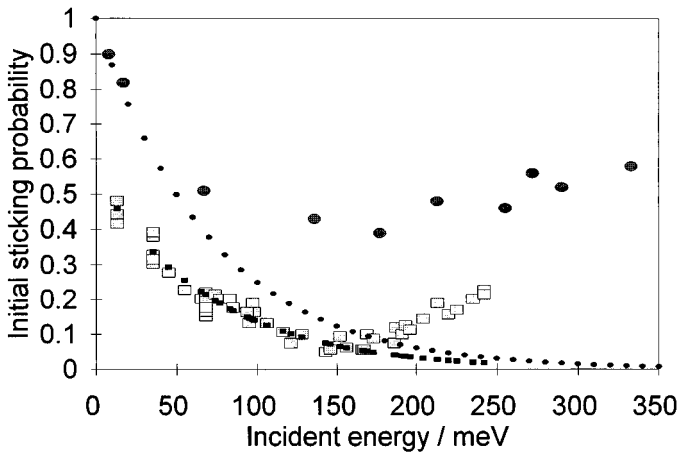

Figure 9. The initial dissociative sticking probability for H_2 on W(100) [14] (●) and W(100)–c(2 × 2)Cu [61] (□). The contribution from the indirect channel to the sticking probability for W(100) (♦) and W(100)–c(2 × 2)Cu (■) has been estimated using the energy dependent exponential decay obtained from the alloy data [61].

The W(100)–c(2 × 2)Cu structure has been the subject of electronic structure calculations [64]. These reveal that there is virtually no alteration in the tungsten electronic density of states upon addition of copper to the W(100) vacancy structure, demonstrating a lack of bonding between the two elements. Concomitantly there is no significant alteration of the copper electronic structure which owes its inert behaviour to the low lying d bands and the absence of states close to E_F [65–67], resulting in a high activation barrier to hydrogen dissociation [18, 24, 35, 37]. There is, however a change in the W(100) electronic structure caused essentially by the c(2 × 2) vacancies, i.e. copper is acting as an inert diluent. This involves the loss of a particularly high density of states on W(100) at or close to E_F observed both experimentally [68] and in calculations [69, 70]. The ensemble responsible for direct dissociation with the lowest barrier is likely to remain a single W atom with an atop trajectory. The main electronic perturbation associated with alloy formation is associated with the W

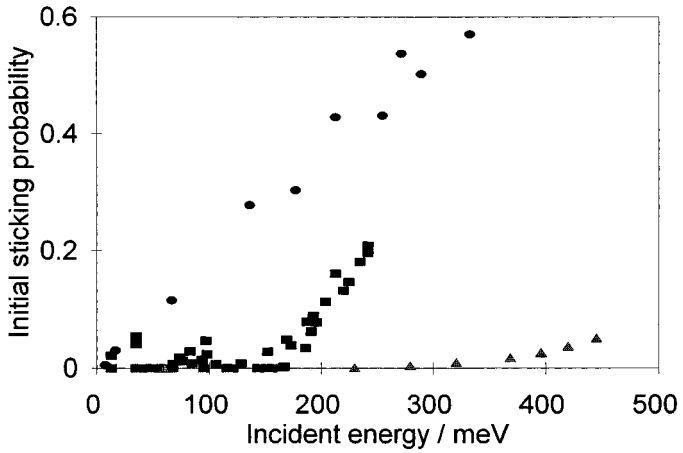

Figure 10. The initial dissociative sticking probability for H_2 in the direct channel on W(100) [14] (●), W(100)–c(2 × 2)Cu [61] (■) and Cu(100) (▲) [20]. The direct channel contributions for W(100) and W(100)–c(2 × 2)Cu have been obtained by subtracting the indirect component from the total sticking probabilities (figure 9).

atoms and results from their missing neighbours, with Cu acting primarily as an inert diluent. The removal of the accessible density of states at W is expected to result in a lower H binding energy and a higher activation barrier as a result of the increased Pauli repulsion, just as is observed experimentally (figure 10). The effect of copper acting as an inert diluent in the W(100)–c(2 × 2)Cu structure is therefore not to change the effective ensemble for dissociation, but to change the electronic structure of the tungsten as a result of the effective reconstruction (induced vacancies) of the W(100) surface.

The dominance of this electronic effect in the change in the activation barrier is also consistent with the even larger depletion of density of states in the region near E_F induced by nitrogen in the W(100)–(2 × 2)N surface. The nitrogen atoms are believed to be adsorbed on fourfold hollow sites in the so called nitride structure. The density of states on W(100)–c(2 × 2)Cu surface was shown to be strongly depleted in the region of 1 eV below and above E_F [64]. The copper atoms themselves make little contribution to these levels since the Cu d band has little density of states within 2 eV of the E_F [64–66]. On the W(100)–c(2 × 2)N surface these electronic states are depleted even further, resulting in a gap of approximately 2 eV between the top of the tungsten d band and E_F [71], very similar to the value found for copper [65]. The activation barrier to dissociation which one can associate with the remaining atop trajectories is found to have a value considerably higher than even W(100)–c(2 × 2)Cu [72], as one may expect on the basis of changes in the electronic structure of W.

2.7. Nitrogen on Cu/W

Both molecular (the α TPD state at 140 K) and dissociative (the β TPD state at 1300 K) adsorption of nitrogen takes place on W(100). The atomic state adsorbs in a c(2 × 2)N structure on W(100) deep in fourfold hollow sites [73]. At low incident translational energies, the dissociative sticking probability is almost constant up to coverages of over half that of saturation, and decreases strongly with surface temperature above 300 K [74]. A kinetic model was constructed on the basis of an accommodated extrinsic precursor state, which could partition between desorption or dissociation. It was later shown using supersonic beams

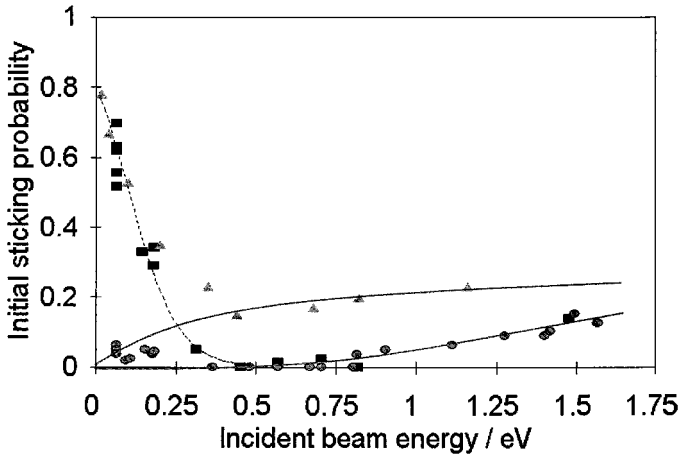

Figure 11. The initial dissociative sticking probability of N_2 on W(100) [75] at 300 K (▲) and W(100)–c(2 × 2)Cu [83] at 300–650 K (●). Measurements of the sticking probability on W(100)–c(2 × 2)Cu at 100 K (■) are included [83] to show the additional molecular sticking component (dotted curve) which does not result in dissociation on the alloy surface. The same trapped precursor, however, is responsible for the indirect channel to dissociative adsorption on W(100). The solid lines are the direct channel to dissociative adsorption on *W*(100) and W(100)–c(2 × 2)Cu.

[75] that, in addition to the precursor mediated channel prevalent at low energies, a direct channel to dissociation could be accessed at higher translational energy. It was also confirmed that the main effect of surface temperature on the precursor mediated channel was to change the partition between desorption and dissociation of the precursor (the difference in the Arrhenius activation energies $E_{des} - E_{diss} = 15.4$ kJ mol^{-1}, and that the trapping probability of the molecule was relatively insensitive to surface temperature. In addition it was found that trapping into both the intrinsic and extrinsic precursors was the same below incident energies of 100 meV, perhaps a result of trapping some distance from the surface where adsorbate effects are small [75]. At higher energies, trapping of the extrinsic precursor was influenced by a changing effective mass due to the adsorbate.

Nitrogen dissociation on copper is highly activated, and adsorption cannot be achieved by thermal or supersonic beam sources, only by exposure to N atoms [76]. Atomic nitrogen adsorbs on all three low index surfaces with a sticking probability near unity, to form a highly stable, nitride surface with a structure similar to that of Cu_3N(111). On Cu(100) nitrogen atoms form c(2 × 2) islands, with N atoms sitting deep in fourfold hollow sites on a reconstructed copper surface [77, 78]. Both Cu(110) [79] and Cu(111) [80] form a similar Cu_3N overlayer, the driving force apparently being the stability of the fourfold co-ordinated N species. Recombinative desorption from Cu(111) generates vibrationally ($T_{vib} = 5100$ K) and translationally excited N_2 ($E_{trans} = 4$ eV) [81], consistent with direct desorption over a barrier at an extended N_2 separation, just as for H_2 on Cu but with a greatly increased barrier [82].

Experiments on nitrogen adsorption on W(100)–c(2 × 2)Cu showed that atomic nitrogen was stable on the alloy surface, with the β TPD state shifted down to ∼1000 K compared to 1300 K on W(100) [83]. However, dissociative adsorption on the W(100)–c(2 × 2)Cu alloy could not be produced with a thermal source, but only by producing the alloy subsequent to nitrogen dissociation on the W(100) surface [84]. The apparent activation barrier to dissociative nitrogen adsorption on the alloy surface was investigated with a supersonic beam source [83]. A comparison of the dissociative sticking probability of nitrogen on

W(100) and W(100)–c(2 × 2)Cu is shown in figure 11. The results showed that there was an increase in the onset of dissociative sticking in the direct channel from <0.1 eV on W(100) to 0.6 eV on the alloy. In addition, the increase in activation barrier in the direct channel was concomitant with the removal of the precursor mediated channel characteristic of W(100) on the W(100)–c(2 × 2)Cu surface [83]. The question as to whether the indirect (precursor mediated) channel on the alloy was removed because of the destabilization of the molecular precursor causing a reduction of the molecular trapping probability, or due to a change in the partition between desorption and dissociation of the accommodated precursor was also addressed. The molecular state exhibits a slight increase in desorption temperature on formation of the alloy, from 150 K on W(100) to 200 K on W(100)–c(2 × 2)Cu. It was shown that the trapping probability of the molecule at low incident energies (where the indirect channel prevails) remains similar on the alloy to that on W(100). Therefore it was concluded that the partition between desorption and dissociation was changed in favour of desorption on W(100)–c(2 × 2)Cu. Since the molecular desorption temperature is increased on the alloy, and recombinative desorption takes place at lower temperature, it is tempting to speculate that this is associated with an increased activation barrier resulting primarily from the atomic (final) state. It is likely that the N atom remains adsorbed in the fourfold hollow site on the alloy, since this is the favoured adsorption site on both W(100) and Cu(100)

3. Conclusion

We have considered the factors which influence the dissociation of hydrogen and nitrogen on a number of alloy surfaces. This has been approached by considering how the potential energy surface in the region of the transition state for dissociative adsorption is modified on well characterized alloy surfaces with respect to the surfaces of the pure components. This comparison has been made in the light of the experimentally determined ground state chemisorption properties of the molecular (reactant or entrance channel) or atomic (product or exit channel) potential, and electronic structure calculations of both the pure metal and alloy surfaces. By considering the reaction ensemble for the transition state we have attempted to understand the influence of electronic and geometric factors in dissociation on alloy surfaces.

Isolated Pt atoms in Cu(111)–c(2 × 2)Pt provide a reaction ensemble for non-activated hydrogen dissociation similar to those on Pt(111), with copper remaining an inert diluent and little apparent electronic perturbation of the active site. Any electronic perturbation of copper atoms by Pd in the second layer of the CuPd(110)–(1 × 2) does not reduce the considerable activation barrier for hydrogen dissociation associated with copper. However in contrast to the PtCu system, isolated Pd atoms in the top layer of the surface do not retain their ability to dissociate hydrogen, probably as a result of the small amount of change required to completely fill the Pd d band. As for other disordered CuPd surfaces, small clusters of Pd atoms in the top surface of substitutional CuPd(110)–(1 × 1) provide reactive ensembles with properties similar to Pd(111) for hydrogen dissociation. On Pt(111)–(2 × 2)Sn the three-atom Pt ensembles provide sites for non-activated, direct dissociative adsorption, similar to those on Pt(111). An activation barrier associated with the onset of direct dissociation at 300 meV is related to the presence of $PtSn_2$ ensembles found on both Pt(111)–(2 × 2)Sn and Pt(111)–($\sqrt{3} \times \sqrt{3}$)R30°Sn alloy surfaces. The formation of an activation barrier for dissociation at the $PtSn_2$ ensemble is shown to correlate with the changes expected in binding energies of the adsorbed product atoms and expectations of the H binding at the transition state based on the ground state energetics. It is also shown that any modification of the pre-exponential associated with alloying must not only take into account changes in the number of reaction sites but also effects associated with the corrugation of the barrier parallel to the surface.

On W(100) the most favoured site for discussion is atop to bridge, with H atoms ending in the most favoured adsorption site, the bridge positions. Formation of the W(100)–(2 × 2)Cu alloy surfaces removes W–W bridge sites and destabilizes adsorbed H, which desorbs at a temperature lower than found on pure copper. The new adsorption site ensemble may be the W–Cu ensemble or may be associated entirely with W. Formation of the alloy is associated with a change from non-activated adsorption on W(100) to activated adsorption, resulting in an onset to direct dissociation at 150 meV. The ensemble responsible for direct dissociation with the lowest barrier is likely to remain a single W atom with an atop trajectory. The main electronic perturbation associated with alloy formation occurs at the W atoms and results from their missing neighbours, with Cu acting primarily as an inert diluent. The increasing barrier to dissociation observed is consistent with the reduction in density of states expected near E_F for a single atom W ensemble. The dominance of this electronic effect in the change in the activation barrier is also consistent with the even larger depletion of density of states in the region near E_F by nitrogen in the W(100)–(2 × 2)N surface. Nitrogen atoms adsorb in fourfold hollow sites and the barrier to dissociation in the atop trajectory is found to have moded even higher.

The activation energy to direct dissociation of nitrogen on W(100) is also low, and in addition an indirect channel is also present. The effect of alloying in the W(100)–(2 × 2)Cu surface is to increase the activation energy to direct dissociation and completely inhibit the indirect channel. This is despite the fact that the trapping of the molecular precursor is unperturbed and indeed the molecular binding energy is slightly increased. It appears that the increased barrier is again correlated with a weakening of the final atomic binding state on the alloy, and is less sensitive to the molecular state potential. This atomic adsorption site is likely to be the same fourfold site as that found on the surfaces of W(100) and Cu(100). It is uncertain whether the lowest activation energy to dissociation is associated with an atop or bridge site trajectory but, if the isolated W ensemble is responsible for nitrogen dissociation, then a similar electronic mechanism can be proposed as in the case of hydrogen.

On all the alloy surfaces described, changes to the dissociation barrier for hydrogen and nitrogen are qualitatively consistent with the modification of the local electronic structure of the reaction ensemble induced by alloying. For direct activated adsorption the barrier to dissociation can be correlated to the binding energies of the final adsorption sites, allowing the dissociation behaviour of different local ensembles to be extrapolated from simple intuitive chemical models of the adsorbate binding energy.

References

[1] Sachtler W M H 1976 *Catal. Rev. Sci. Eng.* **14** 193
[2] Ponec V 1975 *Catal. Rev. Sci. Eng.* **11** 1
[3] Dowden D A 1973 *Proc. 5th Int. Congress on Catal. (Miami, 1972)* vol 1 (Amsterdam: North-Holland) p 621
[4] Bertolini J C 1996 *Surf. Rev. Lett.* **3** 1857
[5] Schneider U, Busse H, Linke R, Castro G R and Wandelt K 1994 *J. Vac. Sci. Technol.* A **12** 2069
[6] Debauge Y, Abon M, Bertolini J C, Massardier J and Rochefort A 1994 *Appl. Surf. Sci.* **90** 15
[7] Rousset J L, Bertolini J C and Miegge P 1996 *Phys. Rev.* B **53** 4947
[8] Christmann K 1988 *Surf. Sci. Rep.* **9** 1
[9] Feibelman P J 1991 *Phys. Rev. Lett.* **67** 461
[10] White J A and Bird D M 1993 *Chem. Phys. Lett.* **213** 422
[11] White J A, Bird D M, Payne M C and Stich I 1994 *Phys. Rev. Lett.* **73** 1404
[12] Hammer B, Scheffler M, Jacobsen K W and Nørskov J K 1994 *Phys. Rev. Lett.* **73** 1400
[13] Rendulic K D, Anger G and Winkler A 1989 *Surf. Sci.* **208** 404
[14] Berger H F, Grosslinger E, Eilmsteiner G, Resch C, Winkler A and Rendulic K D 1992 *Surf. Sci.* **275** L627
[15] Butler D, Hayden B E and Jones J D 1994 *Chem. Phys. Lett.* **217** 423

[16] Gross A, Wilke S and Scheffler M 1995 *Phys. Rev. Lett.* **75** 2718
[17] Kay M, Darling G R, Holloway S, White J A and Bird D M 1995 *Chem. Phys. Lett.* **245** 311
[18] Hammer B and Nørskov J K 1995 *Surf. Sci.* **343** 211
[19] Hayden B E and Lamont C L A 1989 *Phys. Rev. Lett.* **63** 1823
[20] Anger G, Winkler A and Rendulic K D 1989 *Surf. Sci.* **220** 1
[21] Rettner C T, Auerbach D J and Michelsen H A 1992 *Phys. Rev. Lett.* **68** 1164
[22] Healey F, Carter R N, Worthy G and Hodgson A 1995 *Chem. Phys. Lett.* **243** 133
[23] Cottrell C, Carter R N, Nesbitt A, Samson P and Hodgson A 1997 *J. Chem. Phys.* **106** 4714
[24] Hammer B and Nørskov J K 1995 *Nature* **376** 238
[25] Berger H F and Rendulic K D 1991 *Surf. Sci.* **253** 325
[26] Hayden B E, Lackey D and Schott J 1990 *Surf. Sci.* **239** 119
[27] Kratzer P, Hammer B and Nørskov J K 1996 *Surf. Sci.* **359** 45
[28] Darling G R and Holloway S 1995 *Rep. Prog. Phys.* **58** 1595
[29] Hayden B E 1991 *Dynamics of Gas–Surface Interactions* ed C T Rettner and M N R Ashfold (Cambridge: Royal Soc. Chem.) p 137
[30] Murphy M J and Hodgson A 1997 *Phys. Rev. Lett.* **78** 4458
[31] Murphy M J and Hodgson A 1997 *Surf. Sci.* **390** 29
[32] Gross A, Hammer B, Scheffler M and Brenig W 1994 *Phys. Rev. Lett.* **73** 3121
[33] Wiesenekker G, Kroes G J and Baerends E J 1996 *J. Chem. Phys.* **104** 7344
[34] Eichler A, Kresse G and Hafner J 1998 *Surf. Sci.* **397** 116
[35] Harris J and Andersson S 1985 *Phys. Rev. Lett.* **55** 1583
[36] Luntz A C, Brown J K and Williams M D 1990 *J. Chem. Phys.* **93** 5240
[37] Hammer B and Scheffler M 1995 *Phys. Rev. Lett.* **74** 3487
[38] Castro G R, Schneider U, Janssens J and Wandelt K 1992 *Surf. Sci.* **269/270** 321
[39] Linke R, Schneider U, Busse H, Schroeder U, Castro G R and Wandelt K 1994 *Surf. Sci.* **309** 407
[40] Cole R J, Brooks N J, Weightman P, Francis S M and Bowker M 1996 *Surf. Rev. Lett.* **3** 1763
[41] Cottrell C, Bowker M, Hodgson A and Worthy G 1995 *Surf. Sci.* **325** 57
[42] Holmes D J, King D A and Barnes C J 1990 *Surf. Sci.* **227** 179
[43] Rochefort A, Abon M, Delichere P and Bertolini J C 1993 *Surf. Sci.* **294** 43
[44] Noordermeer A, Kok G A and Nieuwenhuys B E 1986 *Surf. Sci.* **172** 349
[45] Newton M A, Francis S M, Li X, Law D and Bowker M 1991 *Surf. Sci.* **259** 45
[46] Newton M A, Francis S M and Bowker M 1991 *Surf. Sci.* **259** 56
[47] Noordermeer A, Kok G A and Nieuwenhuys B E 1986 *Surf. Sci.* **165** 375
[48] P Samson, Nesbitt A, Koel B E and Hodgson A 1998 *J. Chem. Phys.* **109** 3255
[49] Baro A M, Ibach H and Bruchmann H D 1979 *Surf. Sci.* **88** 384
[50] Lee J, Cowin J P and Wharton L 1983 *Surf. Sci.* **130** 1
[51] Janin E, Björkqvist M, Grehk T M, Göthelid M, Pradier C-M, Karlsson U O and Rosemgren A 1996 *Appl. Surf. Sci.* **99** 371
[52] Darling G R and Holloway S 1994 *Surf. Sci.* **304** L461
[53] Gross A 1995 *J. Chem. Phys.* **102** 5045
[54] Hodgson A, Wight A, Worthy G, Butler D and Hayden B E 1993 *Faraday Discuss.* **96** 161
[55] Wight A, Hodgson A, Worthy G, Butler D and Hayden B E 1994 *Surf. Rev. Lett.* **1** 693
[56] Murphy M J and Hodgson A 1998 *J. Chem. Phys.* **108** 4199
[57] White J A, Bird D M and Payne M C 1996 *Phys. Rev.* B **53** 1667
[58] King D A and Thomas G 1980 *Surf. Sci.* **92** 201
[59] Alnot P, Cassuto A and King D A 1989 *Surf. Sci.* **215** 29
[60] Attard G A and King D A 1987 *Surf. Sci.* **188** 589
[61] Butler D and Hayden B E 1995 *Surf. Sci.* **337** 67
[62] Hayden B E and Lamont C L A 1991 *Faraday Discuss. Chem. Soc.* **91** 415
[63] Hayden B E and Gee A T to be published
[64] Singh D and Krakauer H 1989 *Surf. Sci.* **216** 303
[65] Wu S C, Lok C K C, Sokolov J, Quin J, Li Y S, Tian D and Jona F 1989 *Phys. Rev.* B **39** 13 218
[66] Burkstrand J M, Kleiman G G, Tibbetts G C and Tracy J C 1976 *J. Vac. Sci. Technol.* **13** 921
[67] Máca F and Koukal J 1992 *Surf. Sci.* **260** 323
[68] Weng S-L, Plummer G W and Gustafsson T 1978 *Phys. Rev.* B **18** 1718
[69] Pasternak M, Krakauer H, Freeman A J and Koelling d D 1984 *Phys. Rev.* B **29** 5372
[70] Mattheiss L F and Hamann D R 1980 *Phys. Rev.* B **21** 5610
[71] Egawa C, Naito D and Tamaru K 1983 *Surf. Sci.* **131** 49

[72] Hayden B E and Butler D A 1994 *Topics Catal.* **1** 343
[73] Griffiths K, King D A, Aers G C and Pendry J B 1982 *J. Phys. C: Solid State Phys.* **15** 4921
[74] Alnot P and King D A 1983 *Surf. Sci.* **126** 359
[75] Rettner C T, Stein H and Schweizer E K 1988 *J. Chem. Phys.* **89** 3337
Rettner C T, Schweizer E K, Stein H and Auerbach D J 1988 *Phys. Rev. Lett.* **61** 986
Rettner C T, Schweizer E K, Stein H and Auerbach D J 1989 *J. Vac. Sci. Technol.* A **7** 1863
Rettner C T, Schweizer E K and Stein H 1990 *J. Chem. Phys.* **93** 1442
[76] Higgs V, Hollins P, Pemble M E and Pritchard J 1986 *J. Electron Spectrosc. Relat. Phenom.* **39** 137
[77] Leibsle F M and Robinson A W 1993 *Phys. Rev.* B **47** 15 865
[78] Leibsle F M, Dhesi S S, Barrett S D and Robinson A W 1994 *Surf. Sci.* **317** 309
[79] More S, Berndt W, Stampfl C and Bradshaw A M 1997 *Surf. Sci. Lett.* **381** L589
[80] Skelly J F, Munz A W, Bertrams T, Murphy M J and Hodgson A 1998 *Surf. Sci.* **415** 48
[81] Murphy M J, Skelly J F and Hodgson A 1997 *Chem. Phys. Lett.* **279** 112
[82] Murphy M J, Skelly J F and Hodgson A 1998 *J. Chem. Phys.* **109** 3619
[83] Butler D and Hayden B E 1995 *Surf. Sci.* **342** 21
[84] Attard G A and King D A 1990 *J. Chem. Soc. Faraday Trans. 2* **86** 2735